

Decomposition of Octahydro-1,3,5,7-tetranitro-1,3,5,7-tetrazocine," *Journal of Physical Chemistry*, Vol. 86, Oct. 6, 1982, pp. 4260-4265.

¹⁰Karpowicz, R.J. and Brill, T.B., "Kinetic Data for Solid Phase Transition by Fourier Transform Infrared Spectroscopy," *Applied Spectroscopy*, in press.

¹¹Isom, K.B., "A Window Bomb Study of HMX Combustion," CPIA Pub. 261, Vol. 1, Dec. 1974, p. 243.

¹²Derr, R.L., Boggs, T.L., Zurn, D.E., and Dribble, E.J., "Combustion Characteristics of HMX," CPIA Pub. 261, Vol. 1, Dec. 1974, pp. 231-241.

¹³Boggs, T.L., Price, C.F., Zurn, D.E., Derr, R.L., and Dibble, E.J., "The Self-Deflagration of Cyclotetramethylenetetranitramine (HMX)," AIAA Paper 77-859, July 1977.

¹⁴Turnbull, D., "Phase Changes," *Solid State Physics*, Vol. 3, 1956, pp. 226-306.

¹⁵Brill, T.B. and Reese, C.O., "Analysis of Intramolecular Interactions Relating to the Thermophysical Behavior of α , β , and δ -Octahydro-1,3,5,7-tetranitro-1,3,5,7-tetrazocine," *The Journal of Physical Chemistry*, Vol. 84, May 29, 1980, pp. 1376-1380.

¹⁶Kimura, J. and Kubota, N., "Thermal Decomposition Processes of HMX," *Propellants and Explosives*, Vol. 5, Feb. 1980, pp. 1-8 and references therein.

¹⁷Schroeder, M.A., "Critical Analysis of Nitramine Decomposition Data: Activation Energies and Frequency Factors for HMX and RDX Decomposition," *Proceedings of 17th JANNAF Combustion Meeting*, Hampton, Va., Sept. 1980, CPIA Pub. 329, Vol. II, pp. 493-508.

¹⁸Benson, S.W., *Thermochemical Kinetics*, 2nd ed., John Wiley & Sons, New York, 1976, p. 10.

Vibrations of Nonuniform Beams with One End Elastically Restrained against Rotation

P. Vernière de Irassar,*
G. M. Ficcidenti,* and P. A. A. Laura†
Institute of Applied Mechanics,
Puerto Belgrano Naval Base, Argentina

Introduction

THIS Note deals with the determination of the fundamental frequency of the transverse vibration of nonuniform beams with one end elastically restrained against rotation and carrying a mass M at the free end. It is also assumed that the structure is subjected to an axial force F , see Fig. 1.

The analysis is developed by means of the Ritz method on the basis of classical beam theory. Two situations are considered: 1) a linearly tapered beam (Fig. 1a), and 2) discontinuous variation of the cross-sectional area and moment of inertia of the structural element (Fig. 1b).

A review of the recent technical literature reveals that these two cases have not been extensively studied.^{1,3} No claim of originality is made, but it is hoped that design engineers will find the present approach and results useful in their work.

Analysis of the Problem

Linearly Tapered Structural Element

The thickness h and the width b at a position x along the linearly tapered beam as shown in Fig. 1a are given by the

expressions,

$$h = (h_1 - h_0)\bar{x} + h_0, \quad b = (b_1 - b_0)\bar{x} + b_0$$

Then, the cross-sectional area A and the moment of inertia I result in

$$A = A_0(\delta\bar{x} + I)(\gamma\bar{x} + I), \quad I = I_0(\gamma\bar{x} + I)(\delta\bar{x} + I)^3$$

where

$$\bar{x} = x/L, \quad \gamma = \alpha - I, \quad \delta = \beta - I, \quad A_0 = b_0 h_0, \quad \text{and} \quad I_0 = b_0 h_0^3/12$$

with

$$\alpha = b_1/b_0 \quad \text{and} \quad \beta = h_1/h_0$$

(width and thickness ratio, respectively).

In order to obtain an approximate solution by the Ritz method one minimizes the functional, $J[W] = U_{\max} - T_{\max}$ with respect to the arbitrary constants contained in the approximating function (U_{\max} = maximum strain energy, T_{\max} = maximum kinetic energy).

When determining the fundamental mode of vibration, it is convenient to use the approximation⁴

$$W(x) = W_a(x) = C_0(\alpha_{40}\bar{x}^4 + \alpha_{30}\bar{x}^3 + \alpha_{20}\bar{x}^2 + \alpha_{10}\bar{x} + \alpha_{00}) + C_1(\alpha_{41}\bar{x}^5 + \alpha_{31}\bar{x}^4 + \alpha_{21}\bar{x}^3 + \alpha_{11}\bar{x}^2 + \alpha_{01}\bar{x}) \quad (1)$$

which satisfies the boundary conditions,

$$W(I) = 0 \quad (2a)$$

$$\frac{dW}{d\bar{x}} \Big|_{\bar{x}=1} = -\frac{\phi_1 EI_1}{L} \frac{d^2 W}{d\bar{x}^2} \Big|_{\bar{x}=1} \quad (2b)$$

$$\frac{d^2 W}{d\bar{x}^2} \Big|_{\bar{x}=0} = 0 \quad (3a)$$

$$\frac{d^3 W}{d\bar{x}^3} \Big|_{\bar{x}=0} = 0 \quad (3b)$$

Equation (3b) does not take into account the existence of the concentrated inertial force. This approximation considerably simplifies all calculations.

Replacing Eq. (1) in the functional and minimizing it with respect to C_0 and C_1 one obtains, from nontriviality considerations, a frequency equation of the type

$$\begin{vmatrix} C_{11}(\omega) & C_{12}(\omega) \\ C_{21}(\omega) & C_{22}(\omega) \end{vmatrix} = 0 \quad (4)$$

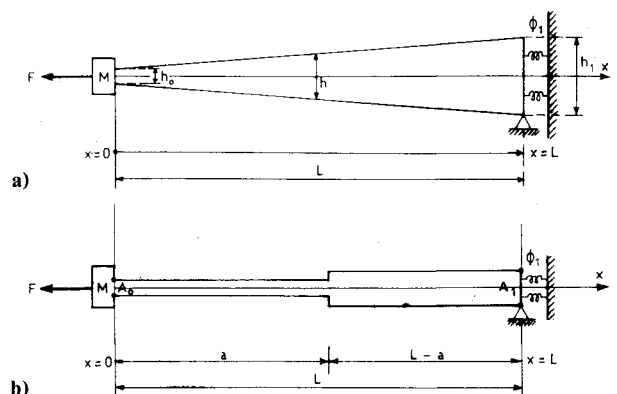


Fig. 1 Vibrating structural elements under study: a) beam with linearly tapered cross section, b) case of discontinuous cross section.

Table 1 Values of $\Omega_0 = \sqrt{(\rho A_0/EI_0)}\omega_0 L^2$ for a beam of constant cross section ($\alpha = \beta = 1$) as a function of $\phi' = (\phi_1 EI_0)/L$ and $\nu = M/M_v (FL^2/EI_0 = 0)$

| $\phi' \backslash \nu$ | 0 | 0.2 | 0.4 | 0.6 | 0.8 | 1 | 2 | Observations |
|------------------------|------|------|------|------|------|------|------|--------------|
| 0 | 3.53 | 2.64 | 2.20 | 1.93 | 1.74 | 1.59 | 1.19 | 1 term |
| | 3.51 | 2.61 | 2.17 | 1.89 | 1.70 | 1.56 | 1.16 | 2 terms |
| | 3.51 | — | 2.16 | — | 1.70 | — | 1.15 | Exact |
| 0.2 | 2.62 | 2.01 | 1.69 | 1.49 | 1.34 | 1.23 | 0.92 | |
| | 2.61 | 1.99 | 1.67 | 1.47 | 1.32 | 1.21 | 0.91 | |
| | 2.61 | — | 1.67 | — | 1.32 | — | 0.90 | |
| 0.4 | 2.17 | 1.68 | 1.42 | 1.25 | 1.13 | 1.04 | 0.78 | |
| | 2.16 | 1.67 | 1.41 | 1.24 | 1.12 | 1.03 | 0.77 | |
| | 2.16 | — | 1.40 | — | 1.12 | — | 0.77 | |
| 0.6 | 1.88 | 1.47 | 1.24 | 1.10 | 0.99 | 0.91 | 0.69 | |
| | 1.88 | 1.46 | 1.24 | 1.09 | 0.99 | 0.91 | 0.68 | |
| | — | — | — | — | — | — | — | |
| 0.8 | 1.70 | 1.32 | 1.12 | 0.99 | 0.90 | 0.83 | 0.62 | |
| | 1.70 | 1.32 | 1.12 | 0.98 | 0.89 | 0.82 | 0.62 | |
| | 1.70 | — | 1.12 | — | 0.89 | — | 0.61 | |
| 1 | 1.55 | 1.21 | 1.03 | 0.91 | 0.82 | 0.76 | 0.57 | |
| | 1.55 | 1.21 | 1.03 | 0.91 | 0.82 | 0.75 | 0.57 | |
| | — | — | — | — | — | — | — | |

Table 2 Fundamental frequency coefficient $\Omega_0 = \sqrt{(\rho A_0/EI_0)}\omega_0 L^2$ of a rigidly clamped beam with continuous variation of the cross section ($\alpha = \beta = 1.2$)

| $\nu = M/M_v \backslash FL^2/EI_0$ | 10 | | 1 | | 0 | | -0.5 | | -1 | |
|------------------------------------|--------|---------|--------|---------|--------|---------|--------|---------|--------|---------|
| | 1 term | 2 terms | 1 term | 2 terms | 1 term | 2 terms | 1 term | 2 terms | 1 term | 2 terms |
| 0 | 7.89 | 7.84 | 5.05 | 5.00 | 4.62 | 4.54 | 4.39 | 4.27 | 4.15 | 3.99 |
| 0.2 | 6.03 | 6.02 | 3.85 | 3.77 | 3.52 | 3.40 | 3.35 | 3.20 | 3.17 | 2.99 |
| 0.4 | 5.06 | 5.06 | 3.23 | 3.14 | 2.96 | 2.84 | 2.81 | 2.67 | 2.66 | 2.49 |
| 0.6 | 4.44 | 4.44 | 2.84 | 2.75 | 2.60 | 2.49 | 2.47 | 2.34 | 2.33 | 2.18 |
| 0.8 | 4.01 | 4.01 | 2.56 | 2.48 | 2.34 | 2.24 | 2.23 | 2.10 | 2.11 | 1.96 |
| 1 | 3.68 | 3.68 | 2.35 | 2.27 | 2.15 | 2.05 | 2.05 | 1.93 | 1.93 | 1.80 |
| 2 | 2.76 | 2.75 | 1.76 | 1.70 | 1.61 | 1.53 | 1.53 | 1.44 | 1.45 | 1.34 |

Table 3 Fundamental frequency coefficient $\Omega_0 = \sqrt{(\rho A_0/EI_0)}\omega_0 L^2$ of a rigidly clamped beam with discontinuous variation of its cross section ($A_0/EI_0 = 0.8$, $I_0/I_1 = 0.64$, $a/L = 0.5$)

| $\nu = M/M_v \backslash FL^2/EI_0$ | 10 | | 1 | | 0 | | -0.5 | | -1 | |
|------------------------------------|--------|---------|--------|---------|--------|---------|--------|---------|--------|---------|
| | 1 term | 2 terms | 1 term | 2 terms | 1 term | 2 terms | 1 term | 2 terms | 1 term | 2 terms |
| 0 | 7.93 | 7.39 | 4.83 | 4.58 | 4.35 | 4.10 | 4.09 | 3.83 | 3.82 | 3.54 |
| 0.2 | 5.96 | 5.76 | 3.63 | 3.49 | 3.27 | 3.12 | 3.08 | 2.91 | 2.87 | 2.68 |
| 0.4 | 4.97 | 4.86 | 3.03 | 2.93 | 2.73 | 2.61 | 2.57 | 2.45 | 2.39 | 2.24 |
| 0.6 | 4.36 | 4.29 | 2.65 | 2.57 | 2.39 | 2.29 | 2.25 | 2.14 | 2.10 | 1.97 |
| 0.8 | 3.92 | 3.87 | 2.39 | 2.32 | 2.15 | 2.06 | 2.03 | 1.92 | 1.89 | 1.77 |
| 1 | 3.60 | 3.56 | 2.19 | 2.13 | 1.98 | 1.89 | 1.86 | 1.77 | 1.73 | 1.63 |
| 2 | 2.69 | 2.67 | 1.64 | 1.59 | 1.47 | 1.42 | 1.39 | 1.32 | 1.29 | 1.21 |

The lowest root of this determinantal equation constitutes the fundamental frequency parameter

$$\Omega_0 = \sqrt{(\rho A_0/EI_0)}\omega_0 L^2$$

Discontinuous Variation of the Cross Section (Fig. 1b)

The procedure is the same in this case. It is convenient to define the parameters,

$$A_0 = b_0 \cdot h_0, \quad A_1 = b_1 \cdot h_1, \quad I_0 = (b_0 \cdot h_0^3)/12$$

$$I_1 = (b_1 \cdot h_1^3)/12$$

Numerical Results and Conclusions

The algebra involved in the determination of the frequency equations is quite simple, but the details are not included here since the expressions are quite lengthy.

On the other hand, the present study contains frequency parameters Ω_0 for a convenient combination of geometric and mechanical parameters. It was also decided to compute buckling loads by setting the frequency coefficient equal to zero in the determinantal equation and then evaluating $P_{cr} = -F$. This was done in order to check the accuracy of the procedure.[‡]

Table 1 shows the value of Ω_0 in the case of a beam of constant cross section in the absence of an axial force. The

[‡]The buckling loads are already available in the literature.⁵ If the values computed following the present approximate procedure are, at least, in fairly good agreement with the exact results available in the literature it seems reasonable to expect that the frequency values determined as a function of an applied axial force will possess sufficient engineering accuracy. The agreement was good for all of the cases considered.

two-term solution yields a fundamental frequency value which is in very good agreement with the one obtained in Refs. 6 and 7 (even the result obtained by means of a one-term solution possesses good engineering accuracy).

Table 2 presents values of Ω_0 for the linearly tapered beam ($\alpha = \beta = 1.2$) rigidly clamped ($\phi' = 0$) for various axial force parameters and mass ratios $\nu = M/M_0$. For $\nu = 0$ the results are in good agreement with the frequency values available in the open literature.⁸

Table 3 contains values of Ω_0 in the case of a structural element with discontinuously varying cross section.

Judging from the accuracy attained in those cases where exact values are available, it seems that the present approach yields useful results when an engineering answer is needed. An inherent advantage of the methodology is the fact that it can be easily implemented on a desk computer.

Acknowledgment

The present investigation has been partially sponsored by Comisión de Investigaciones Científicas (Buenos Aires Province).

References

- Wagner, H. and Ramamurti, V., "Beam Vibrations—A Review," *The Shock and Vibration Digest*, Vol. 9, No. 9, 1977, pp. 17-24.
- Sato, K., "Transverse Vibrations of Linearly Tapered Beams with Ends Restrained Elastically Against Rotation Subjected to Axial Force," *International Journal of Mechanical Sciences*, Vol. 22, No. 2, 1980, pp. 109-115.
- Housner, G. W. and Keightley, W. O., "Vibrations of Linearly Tapered Cantilever Beams," *Journal of Engineering of the Mechanics Division*, ASCE, Vol. 128, Pt. 1, 1963, pp. 1020-1054.
- Laura, P. A. A., Pombo, J. L., and Susemihl, E. A., "A Note on the Vibrations of a Clamped-Free Beam with a Mass at the Free End," *Journal of Sound and Vibration*, Vol. 37, No. 2, 1974, pp. 161-168.
- Timoshenko, S. P. and Gere, J. M., *Theory of Elastic Stability*, 2nd ed., McGraw Hill Book Co., New York.
- Gutiérrez, R. H. and Laura, P. A. A., "Coupled Flexural-Torsional Vibrations of a Beam Elastically Restrained at One End and Carrying a Concentrated Mass at the Other," *Journal of Sound and Vibration*, Vol. 58, No. 2, 1978, pp. 305-309.
- Blevins, R. D., *Formulas for Natural Frequency and Mode Shape*, Van Nostrand Reinhold Company, New York, 1979, p. 163.
- Mabie, H. H. and Rogers, C. B., "Transverse Vibrations of Tapered Cantilever Beams," *Journal of the Acoustical Society of America*, Vol. 51, April 1972, pp. 1771-1774.

Parameters for the Simulation of High Temperature Blown Shock Layers

R. N. Gupta*

NASA Langley Research Center, Hampton, Virginia

Introduction

FOR the Galileo mission to Jupiter, the massive-ablation injection rates (from the probe's forebody heat shield) driven by radiative heating from the high-energy shock-layer gases create a unique flowfield environment.¹ Such an en-

vironment is very difficult to simulate in a ground-based experimental facility. Since all conditions can not be duplicated, care must be taken in what quantities are simulated in an experiment. Holden's² recent work is one of the few experiments applicable to the problem. In this study, he attempted to duplicate a few of the aspects of the entry environment for the stagnation region of the Galileo probe. This work presented many interesting results on the structure and stability of the shock layer over a hemispherical nose-tip body at blowing rates of $0 < \rho_w v_w / \rho_\infty u_\infty < 0.7$ using CF_4 as the principal injectant. Here, ρ_w and ρ_∞ are the wall and freestream values of the density, v_w is the normal injection velocity at the wall, and u_∞ is the freestream velocity. The interpretation of Holden's results, however, requires an analysis of the important parameters in a massively blown re-entry flowfield. The present study explores the impact of the ratios of injection-to-freestream velocity (v_w/u_∞), wall-to-freestream density (ρ_w/ρ_∞), and the shock-layer to ablation-layer gas temperature (T_s/T_w) in simulating the high-temperature blown shock layers. The roles played by these ratios are considered quite important. For example, a larger value of the injection velocity for a given injection rate implies a greater boundary-layer thickness. This, in turn, would entrain more of the high-temperature, radiating gases in the outer portions of the shock layer. These gases would be brought into the lower regions of the shock layer by turbulent diffusion, resulting in higher temperatures close to the body surface for a prescribed surface temperature. Similarly, using a smaller outer shock layer to wall temperature ratio (T_s/T_w) would affect the boundary-layer thickness and entrainment rate.

The purpose of this Note is to evaluate the importance of the velocity, density, and temperature ratios outlined in the previous paragraph. In order to keep the analysis simple, only perfect-gas results for a hydrogen-helium atmosphere are obtained here.

Analysis

For the purpose of analysis, the time-dependent viscous-shock-layer equations of motion³ for a perfect-gas mixture for turbulent flow have been considered. With these equations no-slip boundary conditions are used at the surface and the wall temperature is assigned a constant value. The surface mass injection rate is specified either as a constant value or varied according to the distribution of Fig. 1. The boundary conditions at the shock are calculated by using the shock relations. A two-layer eddy-viscosity model⁴ consisting of an inner law based upon Prandtl's mixing length concept and the Clauser-Klebanoff expression for the outer law is used in the present investigation.

The solutions to the governing equations have been obtained by a time-asymptotic two-step finite-difference method due to McCormack.⁵ The details of the vectorized code are given in Ref. 6 and the results have been obtained on the CYBER 203 computer.

Results and Conclusions

As pointed out in the Introduction, the primary purpose of this study is to evaluate the importance of velocity (v_w/u_∞), density (ρ_w/ρ_∞), and shock-layer to ablation-layer gas temperature (T_s/T_w) ratios for the simulation of high-energy blown shock layers. In particular, the role played by these parameters is studied as to their influence on the entrainment of high-temperature outer region gases since this significantly changes the chemical composition and temperature distribution through the shock layer and, in turn, controls the transport of radiative energy to the probe surface.

In this study, attention has been focussed on the spherical portion of the probe. In order to obtain results over a large part of the curved surface, the probe shape with a small half-angle as shown in Fig. 2 has been studied. (Nomenclature used

Received Jan. 11, 1982; revision received May 26, 1982. This paper is declared a work of the U.S. Government and therefore is in the public domain.

*NRC—Senior Research Associate, Aerothermodynamics Branch, Space Systems Division, on leave from IIT, Kanpur, India; Professor, Department of Aeronautical Engineering, Member AIAA.